Structural Analysis of Polymer Thin Films using Tender X-Ray GISAXS; Concept and Design of GISAXS Experiments using Tender X-Ray Energy at BL-15A2

A dedicated diffractometer for grazing-incidence small-angle X-ray scattering (GISAXS) using tender X-rays (2.1–5 keV) was constructed at BL-15A2. GISAXS using hard X-rays is a powerful tool for understanding the nanostructure in both the vertical and lateral directions of thin films, while tender X-ray GISAXS enables depth-resolved analysis as well as a standard GISAXS analysis in thin films. The diffractometer for the tender X-ray GISAXS is composed of four vacuum chambers, and can be converted into the vacuum state from the sample chamber in front of the detector surface. For model experiments using tender X-ray GISAXS with an X-ray energy of 2.40 keV, polystyrene-poly(methyl methacrylate) block copolymer thin films were investigated.

The small-angle X-ray scattering (SAXS) technique is a powerful tool for material science and biological science [1]. For example, it can be applied to polymers, colloids, proteins, foods, metals and inorganic materials. In general, SAXS is measured at low scattering angle, providing structural information in a microscale or nanoscale such as average particle size, shape, and distribution.

Grazing-incidence small-angle X-ray scattering (GISAXS) measurements have been developed as an appropriate method to investigate the nanoscale structure in thin films [1]. In contrast to the standard SAXS method, GISAXS is performed in reflection geometry. Thus, information about the nanostructure in both the vertical and lateral directions of thin films can be acquired simultaneously. It is well known that X-ray penetration depth is strongly affected by changes in X-ray energy and incident angle. By tuning the angle and energy of the incident X-ray beam, GISAXS experiments using tender X-rays might facilitate depth-sensitive analysis perpendicular to the substrate [1-3]. Here, tender X-ray energy refers to the cross-over between hard and soft X-rays, typically ranging from 1 to 5 keV.

BL-15A was constructed in 2013 and has been in operation since 2014 [4]. The experimental hutch in BL-15A is separated into two tandem stations. The upstream and downstream stations are BL-15A1 for XAFS/XRD/XRF experiments and BL-15A2 for SAXS, respectively. One of the greatest features of BL-15A2 is that a diffractometer is installed for GISAXS utilizing tender X-rays from 2.1 keV to 5 keV.

A lower X-ray energy produces a higher X-ray absorption. Thus, in experiments using soft or tender X-rays, the X-rays must pass through under a vacuum or helium atmosphere. A dedicated diffractometer for tender X-ray GISAXS experiments was installed in BL-15A2 [5]. Figure 1 shows a photograph of the diffractometer. In Fig. 1, the right side of the photograph is the upstream side. The diffractometer is composed of four connected vacuum chambers—pinhole, sample stage, vacuum pass, and beamstop chamber—and the inside of this diffractometer can be placed in a vacuum state. PILATUS3 2M, which is a detector designed for use in a vacuum, was used as a detector for the 2D scattering pattern. Because PILATUS3 2M is connected directly to the beamstop chamber, it can be placed in a vacuum state just before the detection surface.

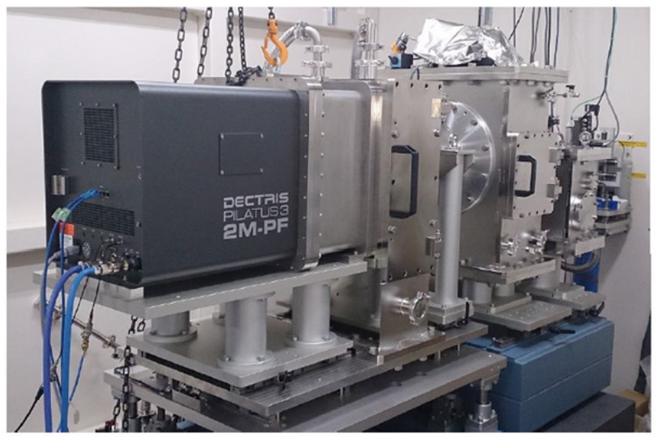

Figure 1: Photograph of the diffractometer for tender X-ray GISAXS.

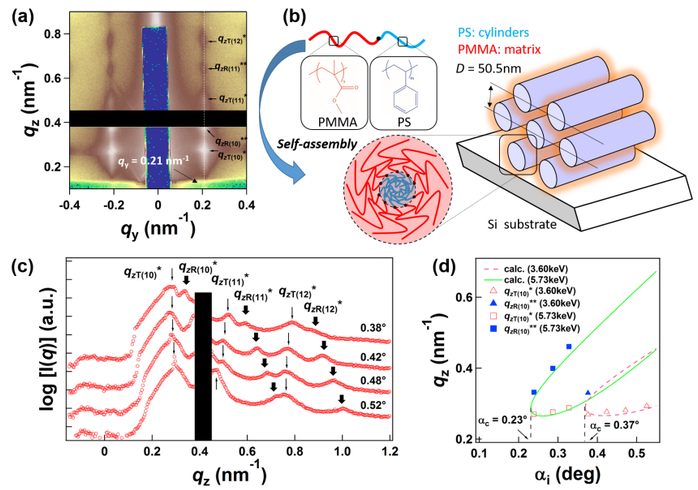

Figure 2: **(a)** Two-dimensional tender X-ray GISAXS image of the PS-PMMA block copolymer thin film (a_i = 0.38°). The incident X-ray energy is 3.60 keV. Thin and thick arrows show the transmitted and reflected parallel oriented hexagonally packed cylinders, respectively. **(b)** Schematic illustration of a PS-PMMA block copolymer (upper-left side) and a cylinder formed by the block copolymer chains (lower-left side). The right side shows the illustration of parallel oriented cylinders. **(c)** One-dimensional SAXS profiles vertically cut around q_y = 0.21 nm^{-1} with various incident angles. **(d)** The a_i dependence of $q_{zT(10)}^*$ and $q_{zR(10)}^{**}$ observed in PS-PMMA at 3.60 keV and 5.73 keV. The solid line shows the theoretical scattering positions using eq. (1).

The 2D-GISAXS pattern of the polystyrene-poly(methyl methacrylate) block copolymer (PS-PMMA) thin film is shown in Fig. 2a [5]. The incident X-ray energy is 3.60 keV (incident angle (α_i) = 0.38°). Figure 2b shows a schematic representation of a PS-PMMA diblock copolymer (upper-left side) [(inset) chemical structures of PS and PMMA blocks] and a cylinder formed by the block copolymer chains (lower-left side). Many diffraction spots are observed in Fig. 2a along the q_z direction around q_y = 0.21 nm^{-1}. All spots were assigned to parallel oriented hexagonally packed cylinders. A schematic illustration of parallel oriented cylinders is shown in Fig. 2b (right side). $q_{zT(10)}^*$ and $q_{zR(10)}^{**}$ denote the transmitted and reflected first-order peak positions of the hexagonally packed cylindrical structures arising from the (10) plane, respectively. The 1D scattering profiles vertically cut at around q_y = 0.21 nm^{-1} with various α_i are shown in Fig. 2c. While the transmitted peaks are shifted slightly to the low-q side with increasing α_i, the reflected ones are moved to the high-q side as α_i increases. Here, let us consider the distorted wave Born approximation (DWBA) theory. Because the incident and scattered X-rays are reflected on the substrate, DWBA must be considered in the q_z direction. The scattering peaks due to the transmitted and reflected X-rays at the substrate can be calculated as

$$q_z = \frac{2\pi}{\lambda}\sin\alpha_i + \sqrt{\left(\frac{2\pi}{\lambda}\sin\alpha_c\right)^2 + \left[\left(\frac{2\pi m}{D}\right) \pm \sqrt{\left(\frac{2\pi}{\lambda}\sin\alpha_i\right)^2 - \left(\frac{2\pi}{\lambda}\sin\alpha_c\right)^2}\right]^2} \quad (1)$$

where m represents the peak order, α_c the critical angle, and D the domain spacing. The plus and minus signs in the equation mean the peak of the transmitted and reflected beams, respectively. Figure 2d represents the α_i dependence of $q_{zT(10)}^*$ and $q_{zR(10)}^{**}$ obtained in PS-PMMA at 3.60 keV and 5.73 keV. D is obtained from fitting using eq. (1), giving D = 50.5 nm (see Fig. 2b). Values of α_{cs} of PS-PMMA at 3.60 keV and 5.73 keV are 0.37 and 0.23°, respectively. It can be seen in Fig. 2d that the experimental α_i dependence of q_z^* and q_z^{**} and the theoretical one using eq. (1) are in excellent agreement. These results confirm that eq. (1) is also applicable qualitatively to the tender X-ray region.

REFERENCES

[1] S. Sakurai, *Polym. Int.* **66**, 237 (2017).
[2] T. Yamamoto, H. Okuda, K. Takeshita, N. Usami, Y. Kitajima and H. Ogawa *J. Synchrotron Rad.* **21**, 161 (2014).
[3] I. Saito, T. Miyazaki and K. Yamamoto, *Macromolecules* **48**, 8190 (2015).
[4] N. Igarashi, N. Shimizu, A. Koyama, T. Mori, H. Ohta, Y. Niwa, H. Nitani, H. Abe, M. Nomura, T. Shioya, K. Tsuchiya and K. Ito, *J. Phys.: Conf. Ser.* **425**, 072016 (2013).
[5] H. Takagi, N. Igarashi, T. Mori, S. Saijo, Y. Nagatani, H. Ohta, K. Yamamoto and N. Shimizu, *J. Appl. Phys.* **120**, 142119 (2016).

BEAMLINE

BL-15A2

H. Takagi[1], N. Igarashi[1], T. Mori[1], S. Saijo[1], Y. Nagatani[1], H. Ohta[2], K. Yamamoto[3] and N. Shimizu[1] ([1]KEK-IMSS-PF, [2] Mitsubishi Electric System & Service Co., Ltd, [3] Nagoya Inst. of Tech.)